NASA TECHNICAL NOTE

NASA TN D-7334

NASA TN D-7334

THE CONTROL OF CARBON DIOXIDE CRYODEPOSITS

by Ellsworth L. Sharpe

Langley Research Center
Hampton, Va. 23665

NATIONAL AERONAUTICS AND SPACE ADMINISTRATION • WASHINGTON, D. C. • NOVEMBER 1973

1. Report No.	2. Government Accession No.	3. Recipient's Catalog No.
NASA TN D-7334		

4. Title and Subtitle	5. Report Date
THE CONTROL OF CARBON DIOXIDE CRYODEPOSITS	November 1973
	6. Performing Organization Code

7. Author(s)	8. Performing Organization Report No.
Ellsworth L. Sharpe	L-8884
	10. Work Unit No.
9. Performing Organization Name and Address	501-22-06-01
NASA Langley Research Center Hampton, Va. 23665	11. Contract or Grant No.
	13. Type of Report and Period Covered
12. Sponsoring Agency Name and Address	Technical Note
National Aeronautics and Space Administration Washington, D.C. 20546	14. Sponsoring Agency Code

15. Supplementary Notes

16. Abstract

An experimental study has been conducted to investigate the parameters affecting the cryodeposition of carbon dioxide frost. In the investigation carbon dioxide frost was cryodeposited from a helium-carbon dioxide mixture into a layer of fibrous insulation surrounding a cylindrical cryogenic tank. Results of the study indicated that not only did deposition occur on the frost surface but also within the frost layer. Over the range of variables investigated both the frost density and the mass of frost deposited were most sensitive to the time of deposition, the percent of carbon dioxide in the purge-gas mixture, and the thickness of the insulation. Frost density and mass of frost deposition were found to increase with time and percent carbon dioxide, and to decrease with increasing insulation thickness.

17. Key Words (Suggested by Author(s))	18. Distribution Statement
Cryodeposition Carbon dioxide frost Thermal protection systems Diffusion Thermodynamics Condensation	Unclassified – Unlimited

19. Security Classif. (of this report)	20. Security Classif. (of this page)	21. No. of Pages	22. Price*
Unclassified	Unclassified	30	Domestic, $3.00 Foreign, $5.50

*For sale by the National Technical Information Service, Springfield, Virginia 22151

THE CONTROL OF CARBON DIOXIDE CRYODEPOSITS

By Ellsworth L. Sharpe
Langley Research Center

SUMMARY

Previous work with a carbon dioxide frost thermal protection system for liquid hydrogen tankage for hypersonic vehicles has indicated that it is important to control both the quantity and quality of cryodeposited frost. Therefore, an experimental study has been conducted to investigate the parameters affecting the cryodeposition of frost. In the investigation carbon dioxide frost was cryodeposited from a helium-carbon dioxide mixture into a layer of fibrous insulation surrounding a cylindrical cryogenic tank. Among the variables examined were: insulation thickness (from 1.65 to 4.19 cm (0.65 to 1.65 in.)); insulation density (between 22.4 and 44.8 kg/m^3 (1.4 to 2.8 lb/ft^3)); percent of carbon dioxide in the two-gas purge mixture (from 5 to 50 percent); total purge-gas pressure (from 3.5 kPa above ambient (0.5 psig) to 103 kPa above ambient (15 psig)); time of deposition (from 25 to 281 min); type of noncondensible gas (helium or nitrogen); temperature of both the cryodeposition chamber (simulated vehicle outer skin) (from 256 to 311 K (461° to 560° R)) and the cryogenic tank (from 20 to 76 K (37° to 137° R)); and tank cooldown rate (from a rate of 5.6 K/min (10° R/min) to more rapid rates). Results of the study indicated that not only did deposition occur on the frost surface but also within the frost layer. Over the range of variables investigated both the frost density and the mass of frost deposited were most sensitive to the time of deposition, the percent of carbon dioxide in the purge-gas mixture, and the thickness of the insulation. Frost density and mass of frost deposited were found to increase with time and percent carbon dioxide, and to decrease with increasing insulation thickness.

INTRODUCTION

A carbon dioxide frost thermal protection system for the liquid hydrogen fuel tanks of hypersonic vehicles was conceived at the Langley Research Center (refs. 1 to 4). This system consists of a layer of fibrous insulation against the tank into which carbon dioxide frost is cryodeposited while the vehicle is on the ground. During flight rapid decompression and aerodynamic heating cause the carbon dioxide frost to sublime. Gas resulting from this sublimation purges the area around the tank during the flight. In addition, heat

that would otherwise be transferred to the fuel and result in boiloff is absorbed as the frost sublimes and transpires through the insulation.

In the tests reported in references 1 to 4, carbon dioxide gas was cryodeposited in the presence of helium which does not condense at liquid hydrogen temperatures. Collisions between molecules as the carbon dioxide diffuses through the stationary layer of helium in the insulation around the fuel tank slow the deposition of the carbon dioxide so that it forms as a frost rather than as hard ice. In the reference studies, some of the variables which affect frost density were considered but not fully investigated. Since CO_2 cannot exist in a liquid phase at the pressures of interest in this investigation (103 kPa above atmospheric (15 psig) and under), prior research concerning deposition of other gases (which can have liquid states) was not directly applicable. Consequently, additional information on the factors affecting the deposition of CO_2 frost is required.

This study was undertaken in order to investigate the parameters which effect the density and mass of carbon dioxide cryodeposits. Carbon dioxide frost was cryodeposited from a helium-carbon dioxide mixture into a layer of fiberglass insulation surrounding a horizontal cylindrical tank which contained cryogenic liquid nitrogen (or, in one case, liquid helium). Tests were conducted varying the insulation thickness, insulation density, time of deposition, type of stationary gas (helium and nitrogen), temperatures of both the simulated vehicle outer surface (outer surface of the cryodeposition chamber) and the cryogenic tank, tank cool-down rate, and both total and partial pressures of the purge gases.

SYMBOLS

Values are given in both SI and U.S. Customary Units. The measurements and calculations were made in U.S. Customary Units.

L	insulation thickness
t	equivalent time of deposition (see eq. (1))
x	frost thickness
β	percent of CO_2 in the purge-gas mixture
Δt	an increment of time
ρ_f	frost density

ρ_i insulation density

ω mass of frost deposited per unit cryogenic-tank area

$\dot{\omega}$ rate of frost mass deposited per unit cryogenic-tank area

Subscript:

c refers to period when tank is fully cooled

MECHANISMS OF FROST DEPOSITION

The sketch in figure 1 illustrates the physical system studied in this paper. Fibrous insulation is shown against a cryogenic tank wall. Frost deposits are shown within the insulation at the wall. Above the insulation is a purge space and an outer surface. The purge space contains a mixture of carbon dioxide and helium. The two main factors which influence both the amount of carbon dioxide deposited and the density of the deposit are heat transfer and diffusion rate.

If the deposition process is controlled entirely by heat transfer, such as would be the case if there was a single condensable gas adjacent to a bare cyrogenic tank, the mass deposition rate is limited only by the ability of the cryogenic fluid to remove heat from the condensing gas. In this process, the condensing gas is deposited as a solid ice, first on the tank wall and then on the surface of the ice as the condensation isotherm moves outward from the tank. As the ice layer builds up on the cryogenic tank the mass deposition rate decreases because of the thermal resistance of the cryodeposited layer. References 1 to 3 discuss tests where 100 percent carbon dioxide purge gas was used. The results of these tests show that carbon dioxide ice with a density of 1666 kg/m^3 (104 lb/ft^3) was formed and the deposition rate decreased with time.

If the deposition process is controlled by diffusion, the mass deposition rate is regulated by the rate at which the condensing gas (carbon dioxide) can diffuse through the insulation and the noncondensable stationary gas (helium). (Helium does not condense at liquid hydrogen temperatures (see ref. 5 and table I).) If the diffusion resistance offered by the noncondensable gas makes the deposition rate slower than that in the case controlled by heat transfer, the condensation isotherm moves outward into the insulation in order to establish thermal equilibrium. The volume between the cryogenic tank and the plane of the condensation isotherm becomes a zone in which condensation can occur. (The insulation and previously deposited frost become nucleation sites for the condensing gas.)

Deposition of solid carbon dioxide particles on nucleation sites randomly spaced throughout a volume will result in the deposition occurring as a frost rather than as a solid ice as in the heat-transfer process. Information supporting this hypothesis is not available in the literature; however, reference 6 indicates that, for an isothermal diffusion process, the rate of mass diffusion is a function of the percent of diffusing gas in the mixture and of the distance over which the diffusion takes place. In the frost-deposition study of this paper the results indicate that the noncondensable gas, trapped within the insulation, provides a stationary-gas layer through which the condensing gas must diffuse.

APPARATUS, INSTRUMENTATION, AND TEST PROCEDURE

The cryodeposition chamber used in this study consisted of two cylindrical aluminum tanks fastened together with C-clamps at a pair of mating flanges. Photographs of the cryodeposition chamber are shown in figure 2. In figure 2(a) the inner or cryogenic tank is clamped inside the outer tank while in figure 2(b) the two tanks are separated. As illustrated the cryogenic tank can be removed easily for measuring frost thickness and weight.

A sketch of the cryodeposition chamber is presented in figure 3. The cryogenic tank is wrapped with fiberglass insulation. During the testing series, insulations from different manufacturers were used and some small differences in results were attributed to the different insulation types. The space between the two tanks (purge space) provides a plenum into which the purge gas is introduced through a copper pipe connected to carbon dioxide and helium bottlefields. A fan was installed in the purge space to mix the incoming gas with the gas already present in the space after early tests had shown that stratification would occur otherwise. Partial-pressure taps extending through the outer tank into the purge space were provided at four stations (top, bottom, and both sides) for monitoring the concentration of the purge gases. These tubes were connected to a gas analyzer in such a manner that the concentrations of individual samples or the average of the four stations could be measured. The gas analyzer, described in reference 7, uses the variation of the ionization potential of different gases in the presence of an alpha-emitting radioactive source to determine the partial pressures of the gases present. In the case of helium and carbon dioxide the digital readout of the partial-pressure gage is accurate to within 0.2 percent. The outer tank is also equipped with a total-pressure gage, a relief valve, and several manual valves for venting the purge space.

The insulation-wrapped cryogenic tank is shown in figure 3 placed in and clamped to the outer tank. The coils outside the tank were used for heating the entering cryogenic coolant in order to control the cool-down rate of the cryogenic tank at the beginning of a test. The flow rate of cryogenic fluid passing through the cryogenic lines is regulated by

the amount of pressure maintained at the supply dewar. After the controlled cool-down period, the cryogenic fluid can be sent directly into the cryogenic tank by opening the bypass valve outside the tank. Inside the tank it passes through another coil. This inner coil has small holes spaced 2.5 cm (1 in.) apart to provide a cryogenic spray which cools the tank wall uniformly. As the test develops, the cryogenic tank fills up with the cryogenic liquid. The vent pipe shown in the drawing allows the gas resulting from the cryogenic boiloff to escape. In order to avoid making penetrations through the cryogenic tank, thermocouple leads from inside the tank were exited through the cryogenic vent pipe. (The thermocouples are placed on the bottom, top, and side of the tank.) Quick-disconnect plugs attached to the thermocouple leads allow separation of the cryogenic tank for measurement purposes. The drain valve attached to the front of the tank is used to empty the tank at the end of a test.

A schematic drawing of the purge-gas supply system and the cryogenic supply system is shown in figure 4.

A photograph of the apparatus can be seen in figure 5. The instrumentation used in the testing program included gas flow meters, an absolute pressure gage, a multichannel temperature recorder, the partial-pressure measuring device, and a balance-type scale for frost-weight measurement.

During the testing series, the test procedure was varied slightly, as indicated in the following paragraphs, when it became obvious that some of the variables listed in references 1 to 4 were no longer important when partial pressure was controlled during frost deposition.

Prior to each test, the cryogenic tank was weighed. (Daily weighings were necessary because the moisture content of the fibrous insulation varied slightly from day to day.) After weighing, the cryogenic tank was placed inside the structural tank and the mating flanges of both tanks were clamped together. A flow of either carbon dioxide or helium was established into the purge space between the two tanks. Gas was allowed to escape from the 6.9 kPa above ambient (1 psig) relief valve until the partial-pressure gage indicated all air had been purged from the purge space. The desired mixture of carbon dioxide and helium was then obtained in the purge space by observing the readout of the partial-pressure gage while the gases were being added.

References 1 to 4 stated that a cool-down rate of 5.6 K (10° R) per minute was desirable in order to deposit frost that was uniform and free from voids; therefore, liquid nitrogen was sent through the exterior copper coil prior to entering the cryogenic tank. The coil could be heated with a forced-hot-air heating gun in order to control the temperature of the incoming coolant. Later in the testing series it was found that if the concentration

of the purge-gas mixture was held constant the cool-down rate was unimportant in frost-density control and the coil was removed from the cryogenic line.

As the tank was cooled down the flow rate of carbon dioxide gas was adjusted to maintain the desired partial and total pressures in the purge space while cryodeposition took place. After a predetermined time (time was one of the test variables) the liquid-nitrogen supply was shut off and the cryogenic tank was emptied. While the liquid nitrogen was being drained from the cryogenic tank, helium was introduced into the purge space so that no further carbon dioxide could be deposited. The helium pressure was maintained at 3.5 kPa (0.5 psig) above room pressure in order to keep air and water vapor out of the purge space.

After the liquid nitrogen was drained from the cryogenic tank the cryogenic tank was removed from the outside tank in order to measure frost weight and thickness. Two weighings (before and after thickness measurement) were made in order to obtain an average weight. (The balance-type scale read to the nearest 5 grams (0.01 lb).) Although only a small amount of the frost weight was lost by sublimation during thickness measurements (less than 2 percent) the use of an average weight during density calculations minimized any resulting error.

A system of 30 probes was used to obtain a rapid measurement of the average frost thickness. As shown in figure 6, a machinist's square was held to the edge of the flange on the cryogenic tank. (Reference marks inscribed on the flange enabled the square to be placed in exactly the same positions during each frost-thickness measurement.) The probes, which were fashioned from metal rods and ordinary binder clamps, were pushed through the insulation until they touched the surface of the frost. The frost was found to have a well-defined surface which was not penetrated by the probes even at densities as low as 320 kg/m^3 (20 lb/ft^3). At this density it had a consistency or texture resembling candle wax. As a point of reference, the more familiar commercial Dry Ice has a density of 721 kg/m^3 (45 lb/ft^3). The distance from the frost surface to the edge of the square was marked off on each probe by adjusting the sliding clamp. This could be done very rapidly with all the measurements being made in only a few minutes, thus minimizing sublimation during measurement. The frost thickness could be determined later from measurements of the clamp position on each probe and knowledge of the initial length taken when no frost was on the tank. The accuracy of the probes is difficult to estimate but on measuring a dry tank individual readings were always within 0.05 cm (0.02 in.) and the average of all the probes would be within 0.025 cm (0.01 in.).

On two separate occasions after the frost was deposited and measured, the tank was heated until a fractional part of the frost was sublimed; the weight and thickness of the remaining frost were again measured in order to determine if the frost density varied throughout its thickness.

During the testing series several variables were investigated. Tests were run varying: insulation thickness (from 1.65 to 4.19 cm (0.65 to 1.65 in.)); insulation density (between 22.4 and 44.8 kg/m^3 (1.4 and 2.8 lb/ft^3)); percent of carbon dioxide in the two-gas purge mixture (from 5 to 50 percent); total purge-gas pressure (from 3.5 kPa above ambient (0.5 psig) to 103 kPa above ambient (15 psig)); time of deposition (from 25 to 271 minutes); type of noncondensible gas (helium or nitrogen); temperature of both the outer tank (from 256 to 311 K (460° to 560° R)) and the cryogenic tank (from 20 to 76 K (37° to 137° R)); and tank cool-down rate (from a rate of 5.6 K/min (10° R/min) to more rapid rates).

RESULTS AND DISCUSSION

Typically, during the tests of this study, as the cryogenic tank was cooled down the inflow of carbon dioxide gas had to be slowly increased in order to hold constant both the total and partial pressures of the purge gases. When the tank was fully cooled and until the completion of a test, the flow rate of carbon dioxide remained essentially constant (in a few of the tests with high carbon dioxide concentrations the condensation rate decreased as much as 5 percent after several hours). The time required to cool the tank down to liquid nitrogen (or liquid helium) temperatures was included in the total deposition time by establishing an equivalent time as the time variable. The equivalent time t was calculated with the following equation:

$$t = \sum_{i=0}^{c} \frac{\dot{\omega}_i \, \Delta t_i}{\dot{\omega}_c} \tag{1}$$

where

$\dot{\omega}_i$ rate of frost mass deposited per unit cryogenic-tank area at some increment of time Δt_i as tank is cooled (where $i = c$ the tank is fully cooled)

c final increment (refers to conditions when the tank is fully cooled)

The quantity $\dot{\omega}_i$ was varied in a stepwise manner over the cool-down period so that this summation could be made.

Carbon Dioxide Concentration and Time

The effects of the percent of carbon dioxide in the purge-gas mixture and time of frost deposition are illustrated in figure 7, which represents the variation of frost mass, thickness, and density as a function of time for a range of carbon dioxide concentrations.

These data, which are for an insulation thickness of 4.19 cm (1.65 in.), are typical of the frost-deposition characteristics encountered throughout the tests.

Figure 7(a) demonstrates the effect of the concentration of carbon dioxide in the purge-gas mixture on the mass of frost deposited. Each line on the graph represents a series of tests at a given concentration of carbon dioxide for different deposition times. It will be noted that the amount of frost deposited varied approximately linearly with time for each carbon dioxide concentration investigated (i.e., frost deposition rate was constant). Since the mass deposition rate increases with increased carbon dioxide concentration in the purge-gas mixture, figure 7(a) indicates that the frost formation was controlled by diffusion. (See the section entitled, "Mechanisms of Frost Deposition.")

In figure 7(b) (frost thickness vs time) a single curve has been used to represent the general trend of all the data, although, as will be discussed later, the thickness appears to be a weak function of the concentration. The frost-thickness increase was rapid during the early part of a test and, as time passed, the frost-thickness growth decreased.

The decrease in thickness buildup rate in figure 7(b) combined with the constant mass deposition rate in figure 7(a) resulted in an increase of density with time as shown in figure 7(c). This increase in frost density with time combined with visual observations of broken pieces of the frost layer (which indicated that the frost density was uniform throughout the thickness) implies that the cryodeposition occurred within the frost layer as was postulated for diffusion controlled deposition in the section "Mechanisms of Frost Deposition." Further evidence of the frost uniformity was obtained when part of the deposited frost was sublimed by heating the outside of the insulation, and the density was remeasured. As indicated by the results in table II, the final densities were only slightly lower than the original. Figure 7(c) also indicates that frost density increased with increased carbon dioxide concentration. (The dashed lines in fig. 7(c) were obtained from cross plotting the data shown by the solid lines.)

The importance of controlling the concentration was indicated qualitatively in some of the preliminary tests performed prior to the installation of the circulating fan in the purge space (see "Apparatus, Instrumentation, and Test Procedure"). Although the local densities were not measured, it was noted that the texture of the frost formation varied markedly from the top to the bottom of the tank. Partial-pressure measurements of local concentrations for one test with an average CO_2 concentration of 50 percent indicated that the purge gas at the top of the deposition chamber was 25 percent CO_2 whereas that at the bottom was 75 percent CO_2. Based on the data of figure 7(c), a threefold variation in density would be expected for this variation in concentration. With the fan installed, which was the case for all the tests reported herein, the variation of CO_2 concentration throughout the purge space was less than 3 percent.

One objective in controlling deposition by monitoring partial pressure was to have a system that could produce repeatable, predictable results in the presence of leakage such as might occur in a practical application. Several early tests were made where leakage was simulated by opening valves at the top and bottom of the outer tank. In general, little change occurred in the frost deposition when this leakage was introduced. The flagged symbols of figure 7 were for one such test which had a leakage rate equal to 2.6 times the flow required for deposition.

Throughout the investigation cryodeposits on the uninsulated flange at one end of the cryogenic tank were always in the form of a hard dense carbon dioxide ice. These cryodeposits were chipped off the flange and were not measured with the cryodeposits embedded in the insulation. The consistency of the ice on the uninsulated flange did not change with either the percent of carbon dioxide in the purge-gas mixture or the time of deposition. Because of the lack of insulation on the flange, the diffusion distance apparently was not sufficient to allow diffusion to control cryodeposition and the resulting ice was controlled mainly by heat transfer.

Insulation Thickness

In order to examine the effect of insulation thickness on carbon dioxide cryodeposits, the results of tests with insulation thicknesses of 4.19, 2.84, and 1.65 cm (1.65, 1.12, and 0.65 in.) were compared. Figures 8 and 9 illustrate the effects of insulation thickness on density and mass deposited for different purge-gas mixtures (carbon dioxide-helium). Both frost density and mass of frost deposited are shown to increase with decreased insulation thickness. Once again the results indicate that the cryodeposition was controlled by diffusion because the insulation thickness (the diffusion distance) had a significant effect on both frost density and the mass of frost deposited.

Cryogenic Tank Cool-Down Rate

All of the test results discussed previously were obtained with a slow cool-down rate of the cryogenic tank (<5.6 K/min (10° R/min)) in accordance with the recommendation of references 1 to 4 in order to insure a uniform frost deposit (free from voids, etc.). Since the present study differed from the literature studies in that purge-gas concentrations were controlled throughout an entire test, the effects of cool-down rate were reinvestigated. Figure 10 shows the results of this study. The data obtained with slow tank cool down are represented by the circles while the rapid-cool-down data are represented by the flagged circles. The rapid cool down was limited only by the rate the liquid nitrogen could be supplied to the cryogenic tank and exceeded 11 K/min (20° R/min) in all cases. The test results indicate cool-down rate has no effect on cryodeposit density or mass if purge-space partial pressures remain constant throughout deposition. As a consequence a rapid cool-down rate was used for all remaining tests.

Total Pressure

Although the total purge-gas pressure was maintained between 3.5 and 6.9 kPa above ambient (0.5 and 1 psig) for most of the tests of this study, several tests were made at a pressure of 103 kPa above ambient (15 psig) to determine the effects of total pressure on frost deposition. In one group of tests the carbon dioxide concentration was held at 20 percent and the deposition time was varied, and in another group the carbon dioxide concentration was varied for a constant deposition time of 200 minutes. Results of these tests are compared with the results obtained at lower total pressure in figures 10 and 11. It is apparent from both figures that the mass and density of the deposited frost are higher at the higher pressure but the increase is small. Consequently, it would be expected that over the total-pressure range of the remainder of the tests, a range which is representative of that for an actual application as a thermal protection system (3.5 to 6.9 kPa above ambient (0.5 to 1 psig)), the effect of total-pressure variation on frost deposition would be small (<1 percent).

Insulation Density

In order to examine the effects of insulation density on frost deposition, the insulation was densified by adding additional layers of insulation and compressing the material to maintain a nominal thickness of 2.67 cm (1.05 in.). The results of tests with two, three, and four layers of insulation with corresponding densities of 22.4, 33.6, and 44.8 kg/m^3 (1.4, 2.1, and 2.8 lb/ft^3) are presented in figure 12. As shown, an increase in insulation density from 22.4 to 33.6 kg/m^3 (1.4 to 2.1 lb/ft^3) lowered the density of the cryodeposits for all carbon dioxide concentrations with the greatest difference occurring at 20 percent carbon dioxide. However, a further increase in insulation density from 33.6 to 44.8 kg/m^3 (2.1 to 2.8 lb/ft^3) produced no change in cryodeposit density. Insufficient information was obtained to assess fully the causes of these density variations. It is apparent, however, from the lack of change of mass deposition with insulation density (see fig. 12(b)) that, over the range investigated, the deposition rate is primarily diffusion controlled.

Outer-Tank Temperature

During a typical test, the temperature of the outer tank, which was exposed to room temperature, would decrease. (For some of the longer tests, temperatures as low as 256 K (460° R) were recorded.) In figure 13 results of tests in which the outer tank was held at 311 K (560° R) throughout an entire test by heating the tank with electrical-resistance heater tapes are compared with results taken from figure 12 for the unheated tank. At the lower carbon dioxide concentrations (10, 20, and 30 percent) the densities of the cryodeposits (see fig. 13(a)) obtained with the heated outer tank (indicated by the

symbols) were higher than the densities for the unheated tank (indicated by the curves); however, for these concentrations the mass of frost deposited (see fig. 13(b)) was not influenced by tank heating. It appears from the consistency of the mass deposition rates that the process is primarily diffusion controlled for these concentrations. The densities are increased because the condensation isotherm moves closer to the cryogenic tank due to the heat addition; consequently, the frost is deposited within a smaller volume. At the highest carbon dioxide concentration (40 percent) the density of the cryodeposit was not influenced by tank heating (see fig. 13(a)), but the mass deposition rate decreased for the heated tank (see fig. 13(b)). It appears that with the heat addition the deposition rate for this concentration is controlled by both heat transfer and diffusion.

Type of Noncondensable Gas

Because of the high cost of helium, an attempt was made to use nitrogen as the noncondensable gas. Although the frost on the sides of the tank was acceptable with nitrogen as the noncondensable gas, the cryodeposits on the top and bottom of the tank were very uneven. The frost layer on the top was very thin, whereas the deposits on the bottom were of very low density (resembling snow) and protruded from the insulation. This condition persisted even when the incoming liquid nitrogen was heated to maintain the cryogenic tank temperature at 117 K (210° R). It was evident that with nitrogen as the noncondensable gas strong convective currents were established. The flow of cold nitrogen down the tank wall and out through the insulation at the bottom caused the condensation isotherm at the bottom to move outward and thereby promoted the formation of low density frost. The effects of convection were much more pronounced with nitrogen than with helium as might be expected from a consideration of their molecular weights. If nitrogen is to be used as a noncondensable gas, physical barriers must be incorporated in the insulation to impede the convective flow.

Cryogenic-Tank Temperature

In one experiment liquid helium was used as the cryogen to obtain an average cryogenic-tank temperature of 21 K (37° R). Results of this experiment are compared with corresponding results obtained with a cryogenic-tank temperature of 77 K (140° R) in figure 14. As can be seen, the mass deposition for the lower temperature (see fig. 14(b)) is approximately 25 percent higher; however, the density (see fig. 14(a)) is not strongly affected. It appears that with the cooler tank wall the condensation isotherm is located nearer the free surface of the insulation and as a consequence of the shorter diffusion distance the deposition rate is increased. The higher deposition rate is offset by the larger deposition volume so that the frost density remains relatively constant.

Repeatability

Table III is a compilation of test results presented to demonstrate the repeatability of deposition properties. The test results are presented in pairs, each of which represents tests which were run with the same, or almost the same, test conditions. The results indicate that frost can be deposited at a prescribed mass and density if the frost-deposition parameters are controlled.

Correlation of Primary Variables

Over the range of variables examined in this study, deposition time, percent of carbon dioxide in the purge-gas mixture, and the thickness of the insulation had the most significant effect on the frost-deposition characteristics. An examination of the data indicated that the mass of frost deposited varied linearly with deposition time and percent carbon dioxide and inversely with the insulation thickness. Figure 15(a) is a plot of the mass of frost deposited per unit area versus percent CO_2 times time of deposition divided by insulation thickness. All data shown previously have been included in the plots of figure 15. There were several different insulations used throughout the study and some small differences between types are apparent. In general, the data follow the straight-line relationship quite well.

Frost thickness was found (by the use of a least squares method of curve fitting) to be proportional to the cube root of the percent of carbon dioxide in the purge-gas mixture multiplied by the square root of the deposition time. In figure 15(b) a plot of this linear relationship is shown. The plots of figure 15 can be used as an estimate of the values of the given parameters to be used to obtain frost deposition at a specified quantity and quality. However, to obtain accurate values for ranges of parameters not included in the present tests, additional deposition tests would be required where all of the parameters that have been identified as having some effect were controlled to their desired values. The use of the two parameters shown in figure 15 should make possible the correlation of the new data and minimize the number of required tests. It will be noted that the above relationships were obtained using carbon dioxide concentrations up to 50 percent and the validity for higher carbon dioxide concentrations is questioned – for example, frost density with a concentration of 100 percent carbon dioxide is always 1666 kg/m^3 (104 lb/ft^3), independent of time (refs. 1 to 4).

CONCLUSIONS

Carbon dioxide frost was cryodeposited within fiberglass insulation around a horizontal cylindrical cryogenic tank while a mixture of carbon dioxide and helium (or other

noncondensable gas) was maintained at constant partial pressures in a purge space around the outside of the insulation. Liquid nitrogen was used as the coolant in the cryogenic tank in all but one of the tests – liquid helium was used at that time. Frost density and mass of frost deposited were the measurements of interest while variables investigated included time of deposition, percent of carbon dioxide in the two-gas mixture, total pressure, the cryogenic tank cool-down rate, insulation thickness and density, the temperature of the outer surface of cryodeposition chamber (simulated vehicle outer skin), and the type of noncondensable gas.

The tests pointed out that both frost mass and density could be predicted if the proper variables were controlled. Frost density and mass deposited were most sensitive to the following parameters: time of deposition, the percent of carbon dioxide, and the insulation thickness.

A detailed list of the specific conclusions of this study is presented below:

1. Both the mass of frost deposited and the density of that deposit increase with deposition time.

2. After an initial rapid increase in the thickness of the frost layer, frost deposition continues within the volume of the frost layer such that the density of the frost was relatively uniform throughout.

3. Both the mass of frost deposited and the density of the deposit increase with the percent of carbon dioxide in the purge-gas mixture.

4. If the percent of carbon dioxide in the purge-gas mixture remains constant during deposition, the cool-down rate of the cryogenic tank does not affect the frost uniformity, density, or mass deposited.

5. A purge-gas pressure of 2 atmospheres results in only a small increase of both frost density and mass of frost deposited when compared with results of tests run at 1 atmosphere.

6. The frost density and frost-mass buildup increase with decreasing insulation thickness.

7. When insulation density was changed from 22.43 to 33.64 kg/m^3 (1.4 to 2.1 lb/ft^3) the frost density decreased; however, when the insulation density was increased from 33.64 to 44.86 kg/m^3 (2.1 to 2.9 lb/ft^3) no change in frost density was observed. The mass of frost did not vary for the three insulation densities considered.

8. If the temperature of the simulated outer vehicle skin was held constant by adding heat, the density of the frost deposits increased while the mass deposited remained constant.

9. The mass of frost deposited increased slightly when the cryogenic-tank temperature was reduced from 77 to 21 K (140° to 37° R).

10. An uneven frost deposit was evident on the lower portion of the tank when nitrogen gas was substituted for helium in the two-gas purge mixture.

11. In correlating the primary variable in the range of variables examined in this study the following relationships were identified:

(a) The mass of frost deposited is proportional to both the percent of carbon dioxide in the purge-gas mixture and the time of deposition and is inversely proportional to the thickness of the insulation.

(b) The frost thickness is proportional to both the cube root of the percent of carbon dioxide in the purge-gas mixture and the square root of the deposition time.

Langley Research Center,
National Aeronautics and Space Administration,
Hampton, Va., August 21, 1973.

REFERENCES

1. Jackson, L. Robert; Davis, John G., Jr.; and Wichorek, Gregory R.: Structural Concepts for Hydrogen-Fueled Hypersonic Airplanes. NASA TN D-3162, 1966.

2. Jackson, L.; and Anderson, S.: A Carbon Dioxide Purge and Thermal Protection System for Liquid Hydrogen Tanks of Hypersonic Airplanes. Advances in Cryogenic Engineering, Vol. 2, Plenum Press, Inc., 1967, pp. 146-156.

3. Jackson, L. Robert; and Sharpe, Ellsworth L.: A Carbon Dioxide Purge and Thermal Protection System for Liquid Hydrogen Tanks. Conference on Hypersonic Aircraft Technology, NASA SP-148, pp. 501-513.

4. Clay, John P.: Carbon Dioxide Frost as Insulation for Hypersonic Spacecraft. Insulation – Materials and Processes for Aerospace and Hydrospace Applications, Soc. Aerosp. Mater. Process Eng., May 1965.

5. Anon.: Cryogenics and Industrial Gases – Data Book and Buyers Guide. Vol. 6, No. 3, May/June 1971.

6. Rohsenow, Warren M.; and Choi, Harry Y.: Heat, Mass, and Momentum Transfer. Prentice-Hall, Inc., 1961.

7. Melfi, Leonard T., Jr.; and Wood, George M., Jr.: The Use of an Ionization Gage as a Quantitative Analyzer for Bi-Gaseous Mixtures. NASA TN D-1597, 1962.

TABLE I.- PHASE-CHANGE TEMPERATURES FOR SEVERAL SUBSTANCES AT ATMOSPHERIC PRESSURE

Substance	Liquefaction temp., K (^{o}R)	Solidification temp., K (^{o}R)
Nitrogen	77 (140)	63 (114)
Hydrogen	20 (37)	14 (25)
Helium	4 (8)	1 (2)
Carbon dioxide	--- ----	194 (350)

TABLE II.- TESTS TO DETERMINE UNIFORMITY OF FROST DEPOSITS

Unit mass				Density			
Initial		Final (a)		Initial		Final (a)	
kg/m^2	(lb/ft^2)	kg/m^2	(lb/ft^2)	kg/m^3	(lb/ft^3)	kg/m^3	(lb/ft^3)
6.84	(1.40)	4.32	(0.88)	465	(29.0)	416	(26.0)
9.72	(1.99)	5.27	(1.08)	580	(36.2)	543	(33.9)

[a]Final properties as measured after sublimation of approximately half the original frost deposit.

TABLE III.- REPEATABILITY OF RESULTS FOR FROST DENSITY AND MASS

Insulation thickness, cm (in.)	Percent CO_2	Deposition time, min	Unit mass, kg/m^2 (lb/ft^2)	Density, kg/m^3 (lb/ft^3)
3.89 (1.53)	20	122	6.10 (1.25)	420 (26.2)
3.89 (1.53)	20	122	6.10 (1.25)	416 (26.0)
3.89 (1.53)	20	117	6.44 (1.32)	447 (27.9)
3.89 (1.53)	20	116	6.54 (1.34)	452 (28.2)
4.19 (1.65)	10	205	5.47 (1.12)	421 (26.3)
4.19 (1.65)	10	206	6.15 (1.26)	415 (25.9)
4.19 (1.65)	40	50	6.93 (1.42)	633 (39.5)
4.19 (1.65)	40	50	6.30 (1.29)	602 (37.5)
2.63 (1.035)	20	180	5.61 (1.19)	774 (48.3)
2.63 (1.035)	20	183	6.15 (1.26)	758 (47.3)

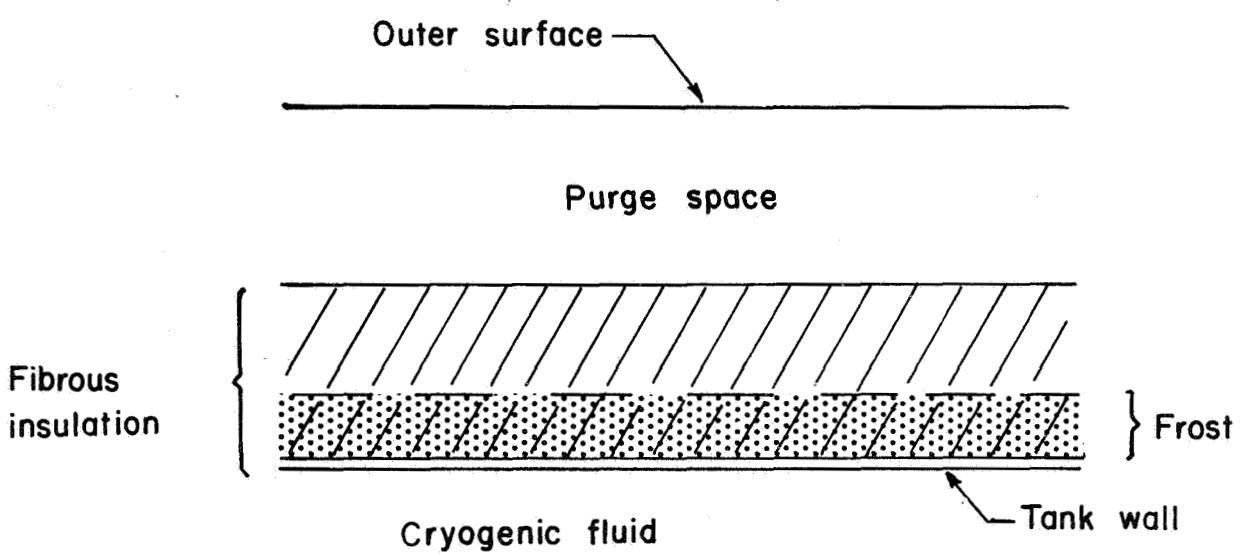

Figure 1.- A sketch of the physical system studied.

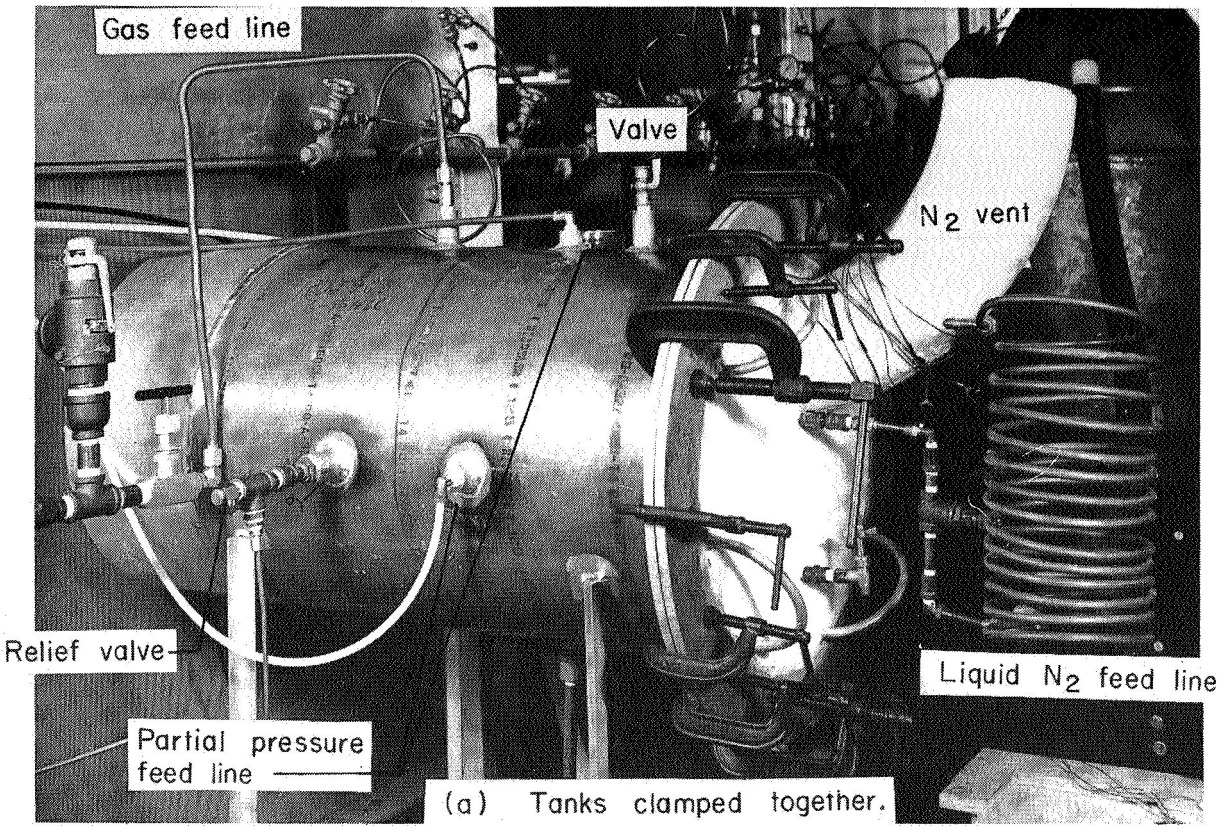

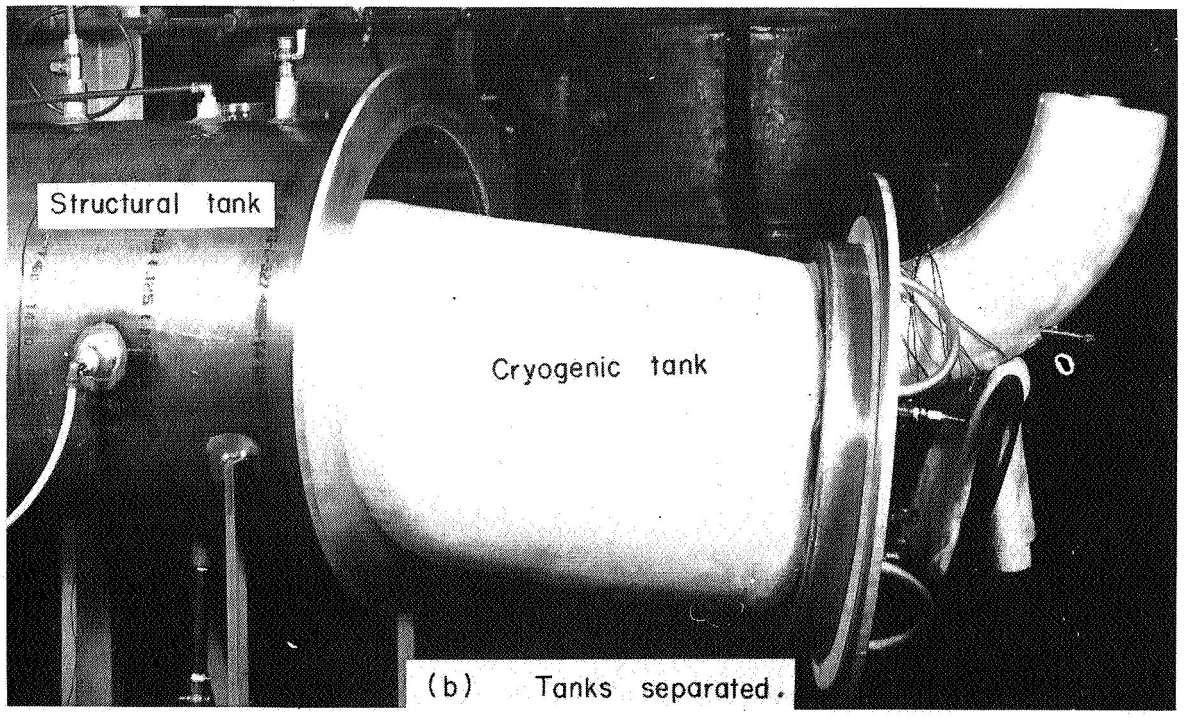

L-73-6824

Figure 2.- Photographs of the cryodeposition chamber.

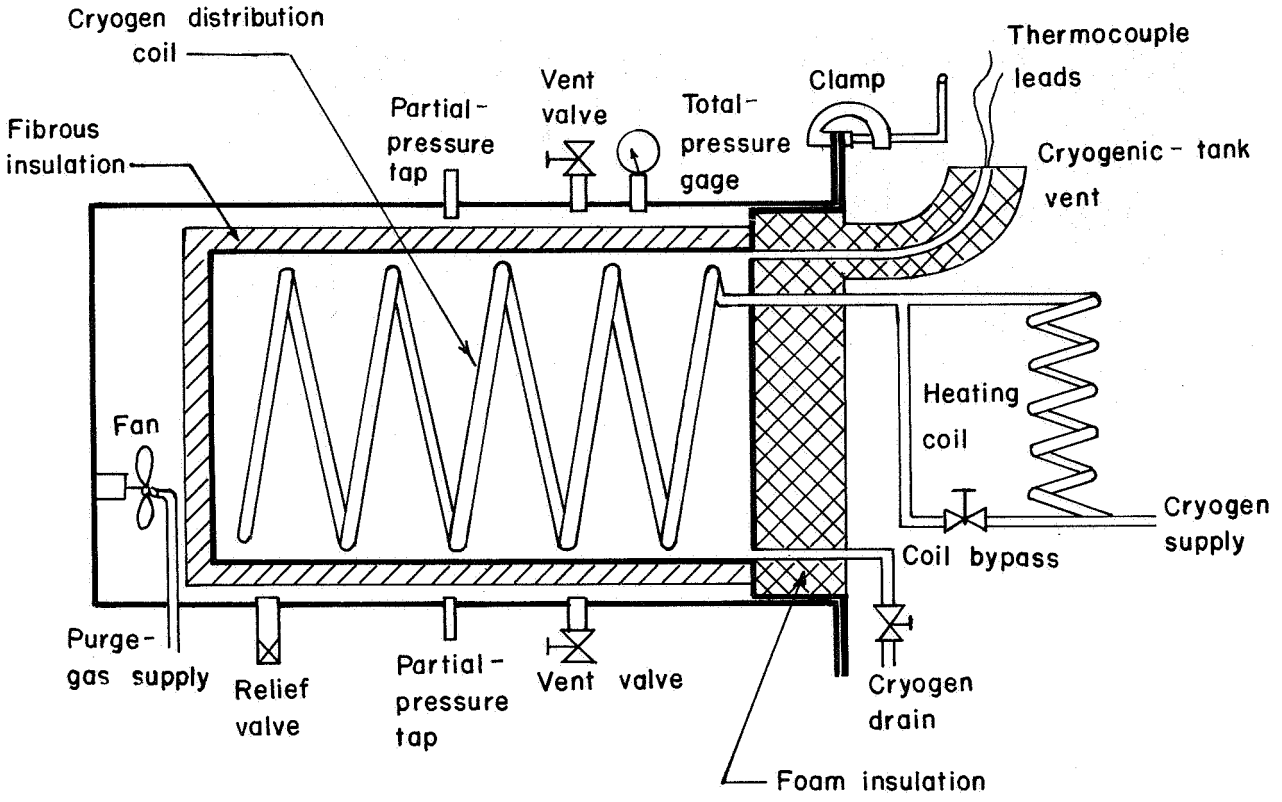

Figure 3.- Cross-sectional sketch of the cryodeposition chamber.

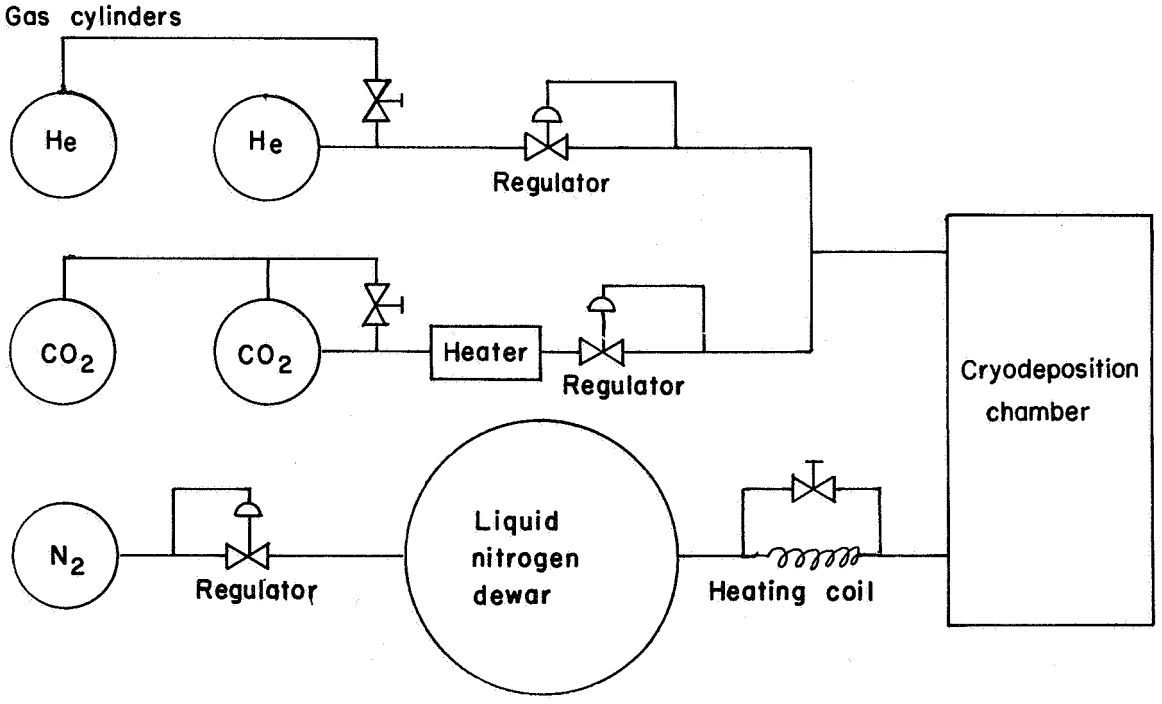

Figure 4.- A schematic drawing of the purge-gas and cryogenic supply systems.

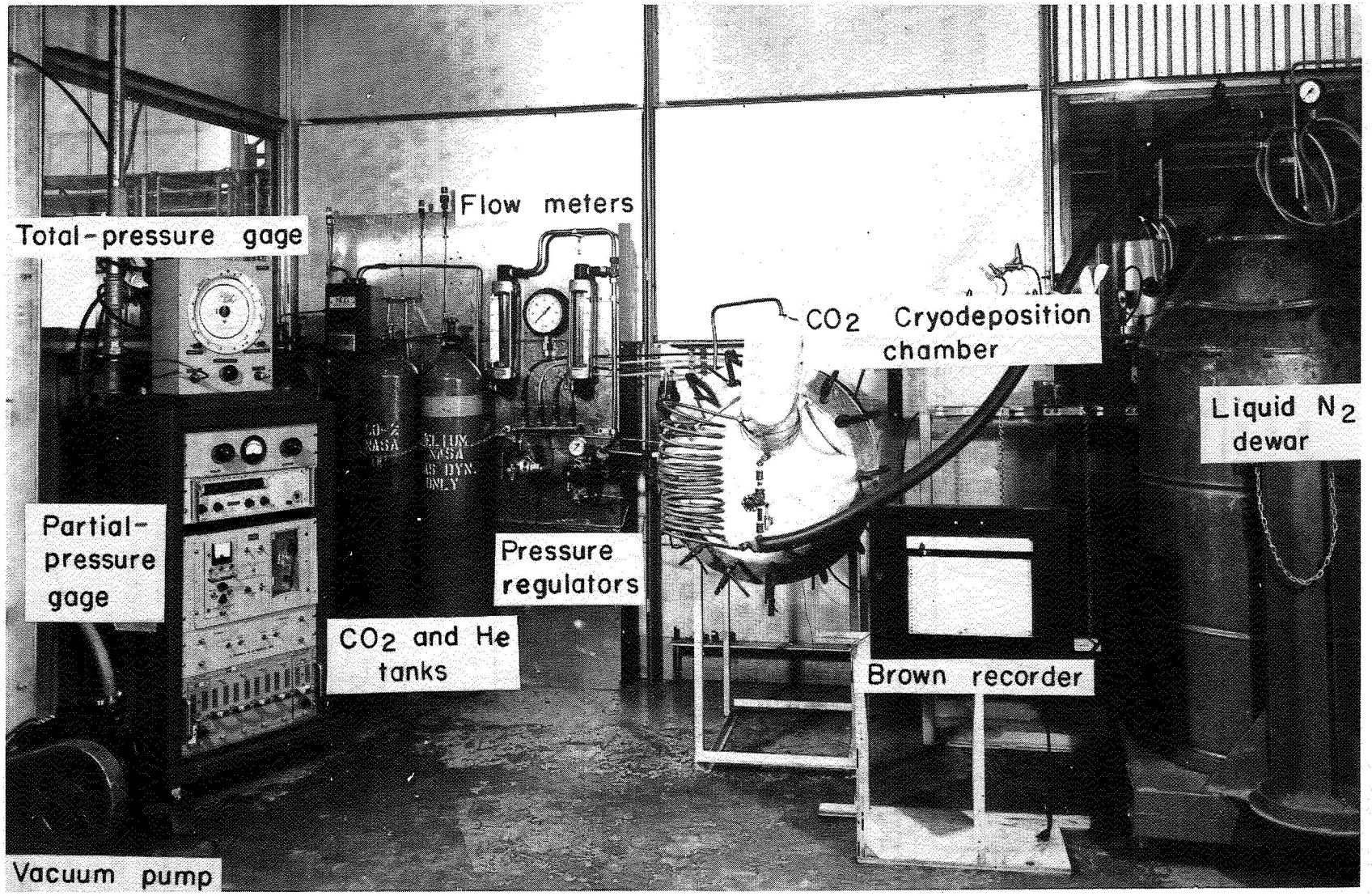

L-66-5045.1

Figure 5.- Photograph of the test apparatus.

L-68-3345

Figure 6.- A photograph of frost measurement in progress.

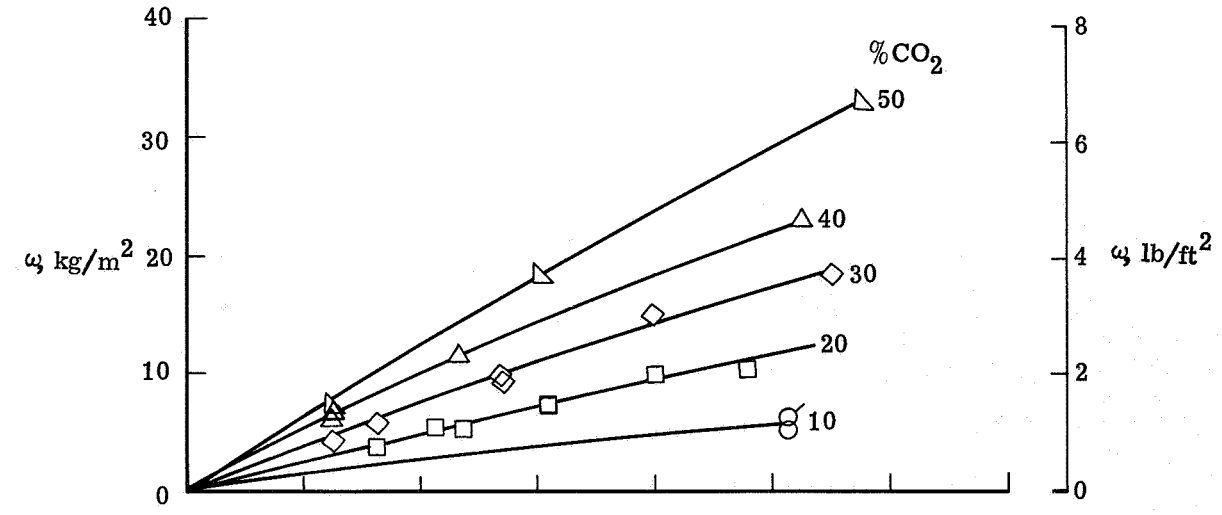

(a) Mass versus time.

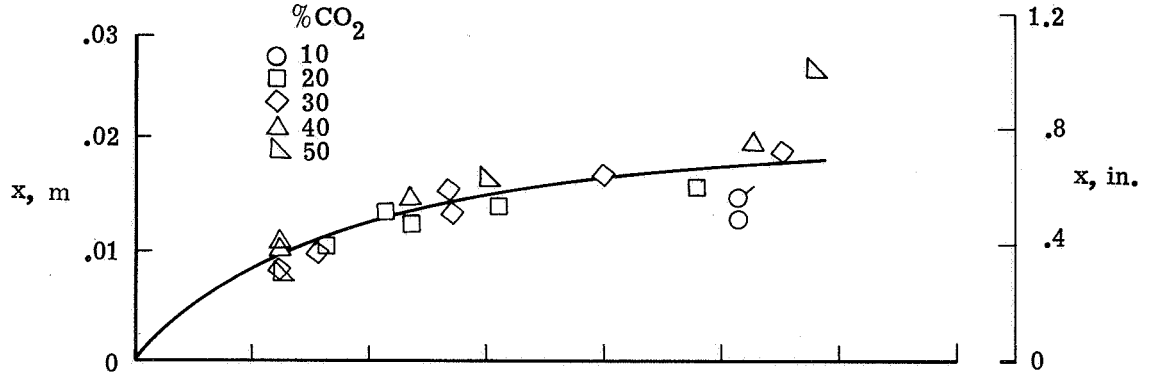

(b) Frost thickness versus time.

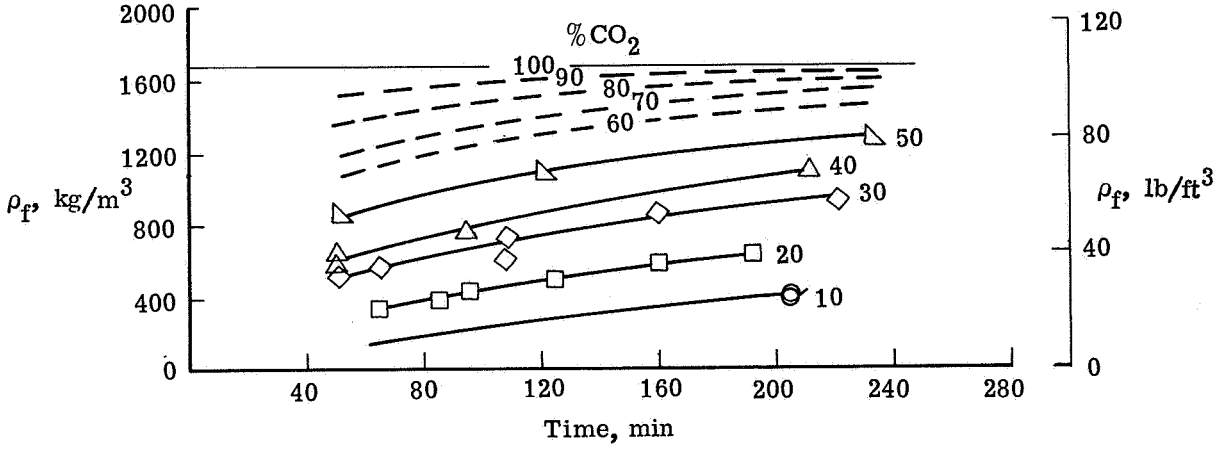

(c) Density versus time.

Figure 7.- The effects of deposition time and percent of CO_2 in the purge gas on carbon dioxide cryodeposits. Flagged symbols represent test with simulated leaks. L = 4.19 cm (1.65 in.); ρ_i = 22.4 kg/m^3 (1.4 lb/ft^3).

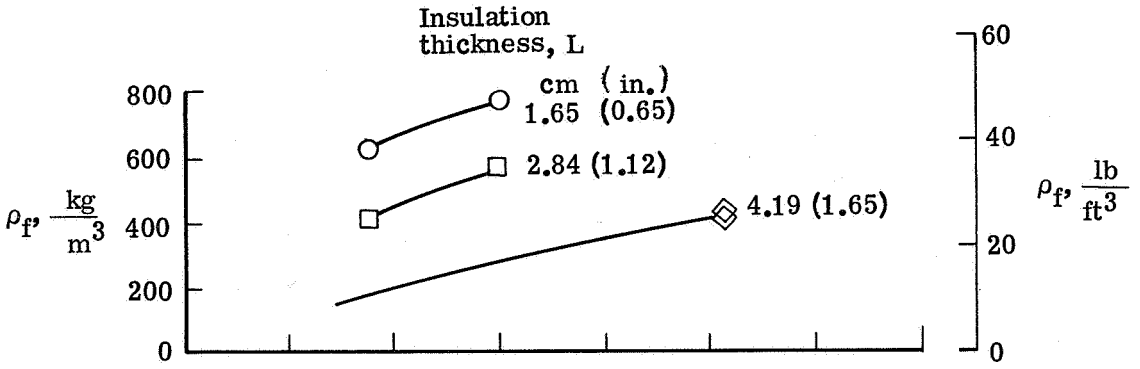

(a) 10 percent CO_2.

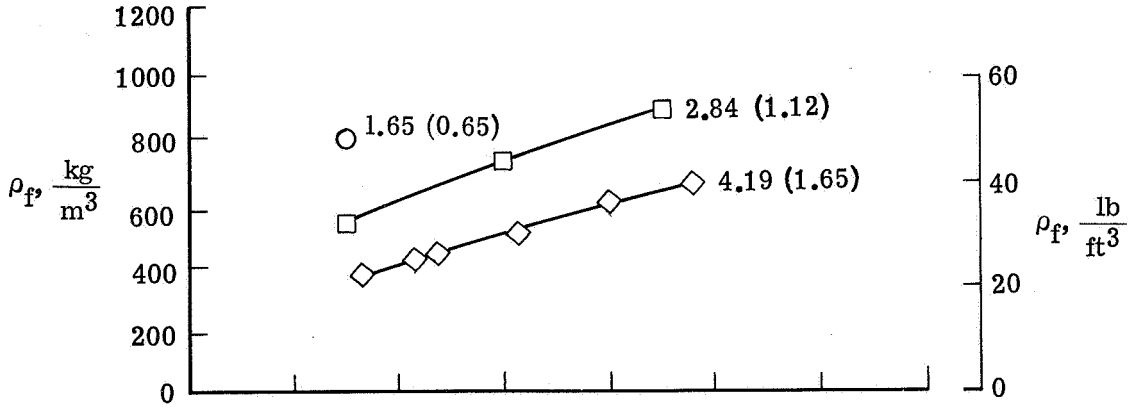

(b) 20 percent CO_2.

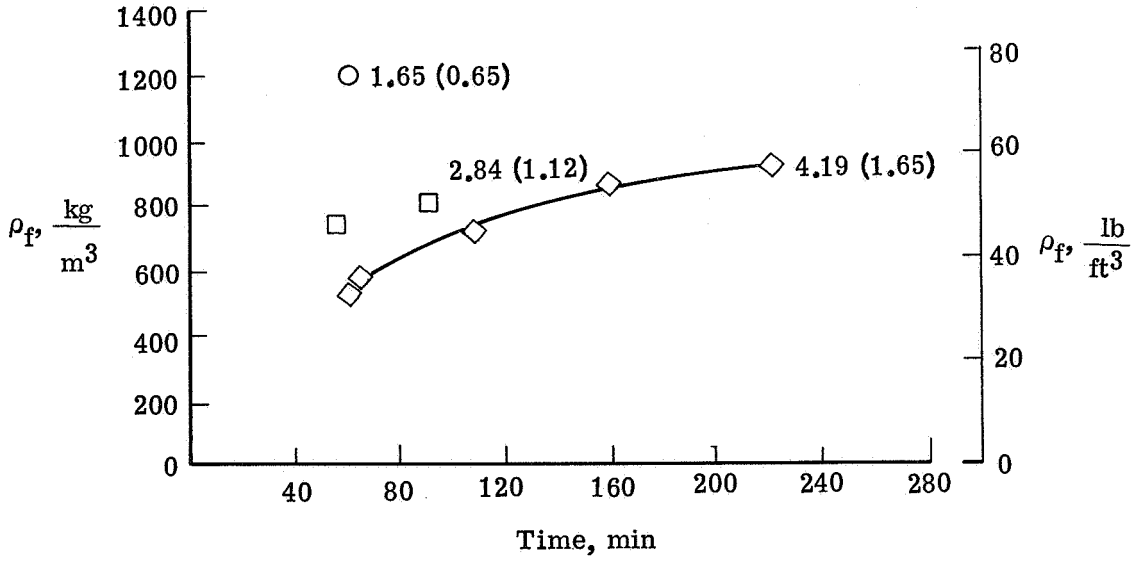

(c) 30 percent CO_2.

Figure 8.- Effects of insulation thickness on frost density. ρ_i = 22.4 kg/m^3 (1.4 lb/ft^3).

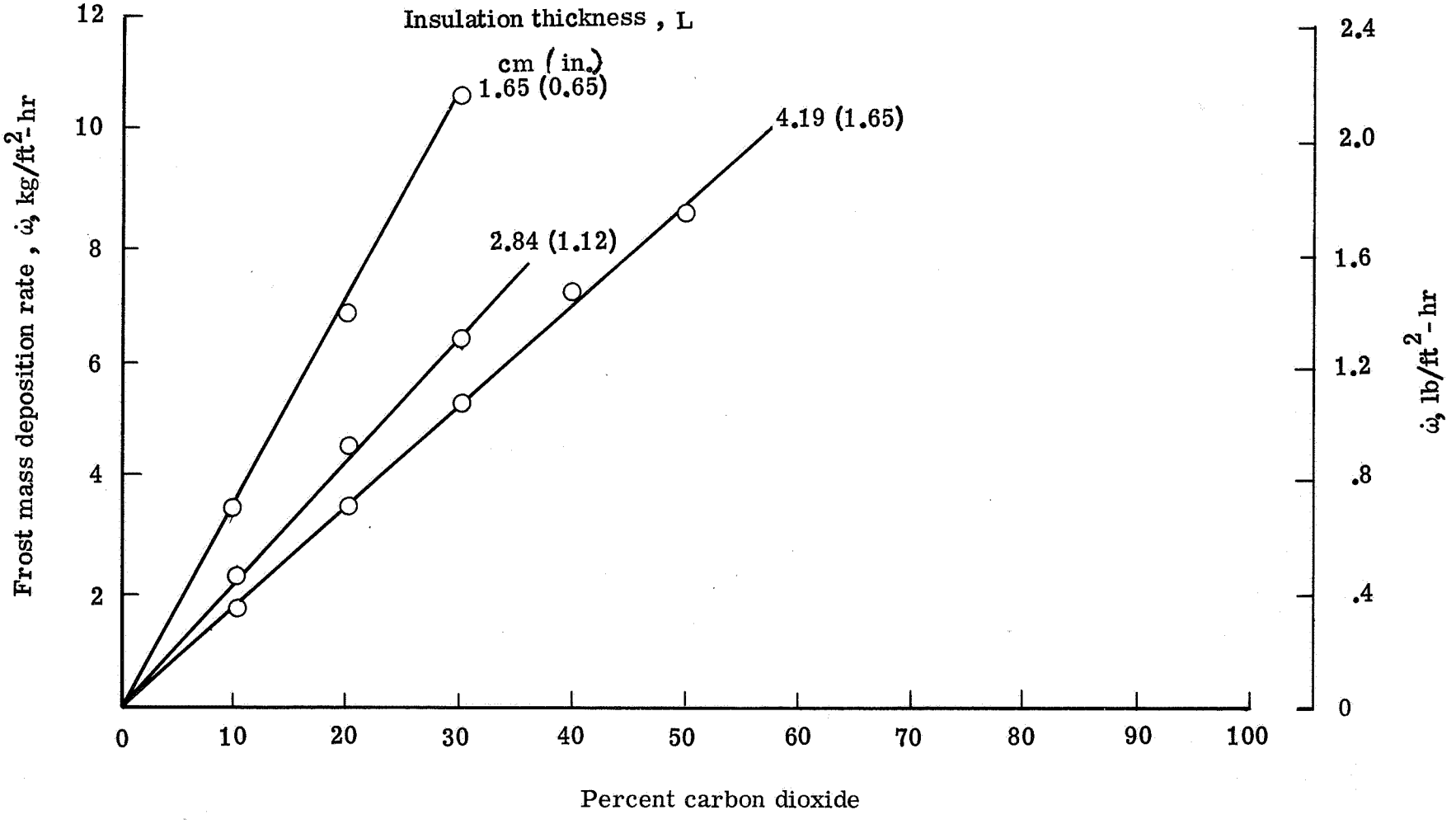

Figure 9.- The effect of insulation thickness on frost mass deposition rate. ρ_i = 22.4 kg/m^3 (1.4 lb/ft^3).

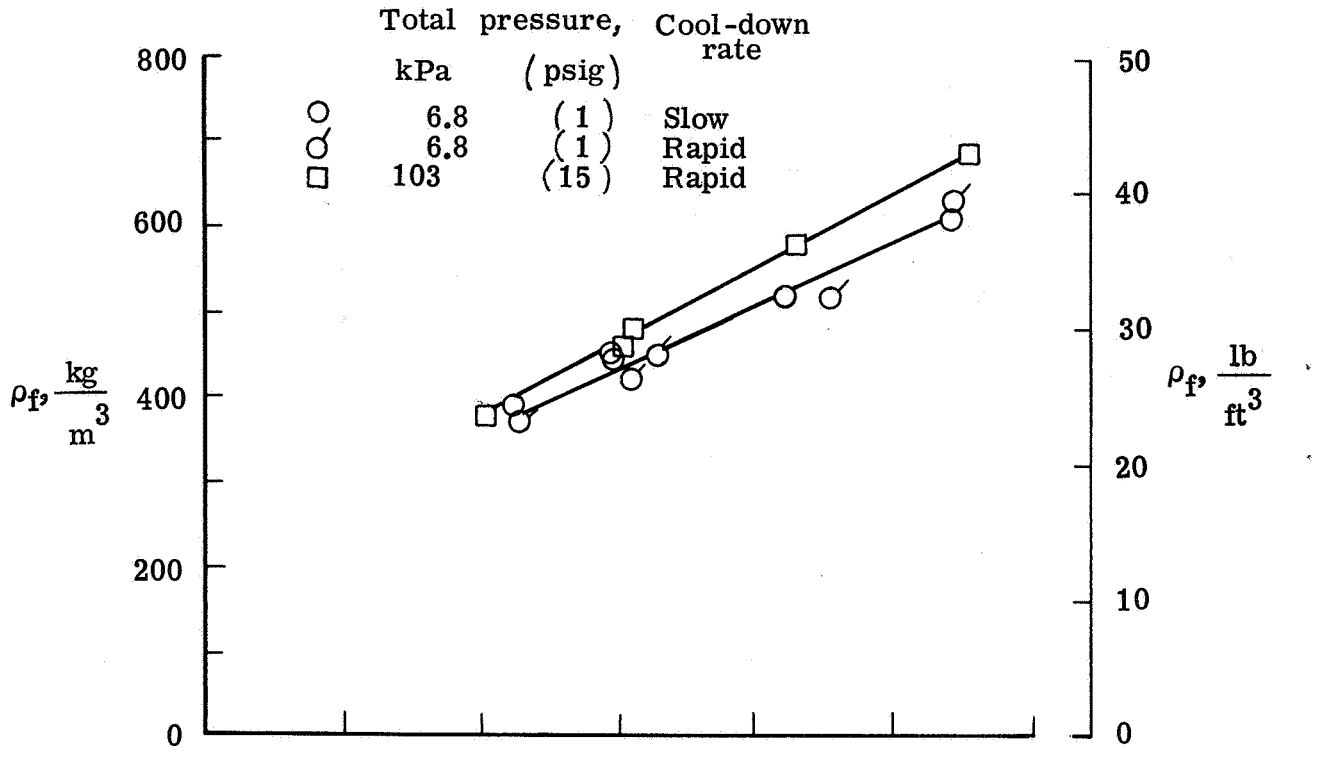

(a) Density versus time.

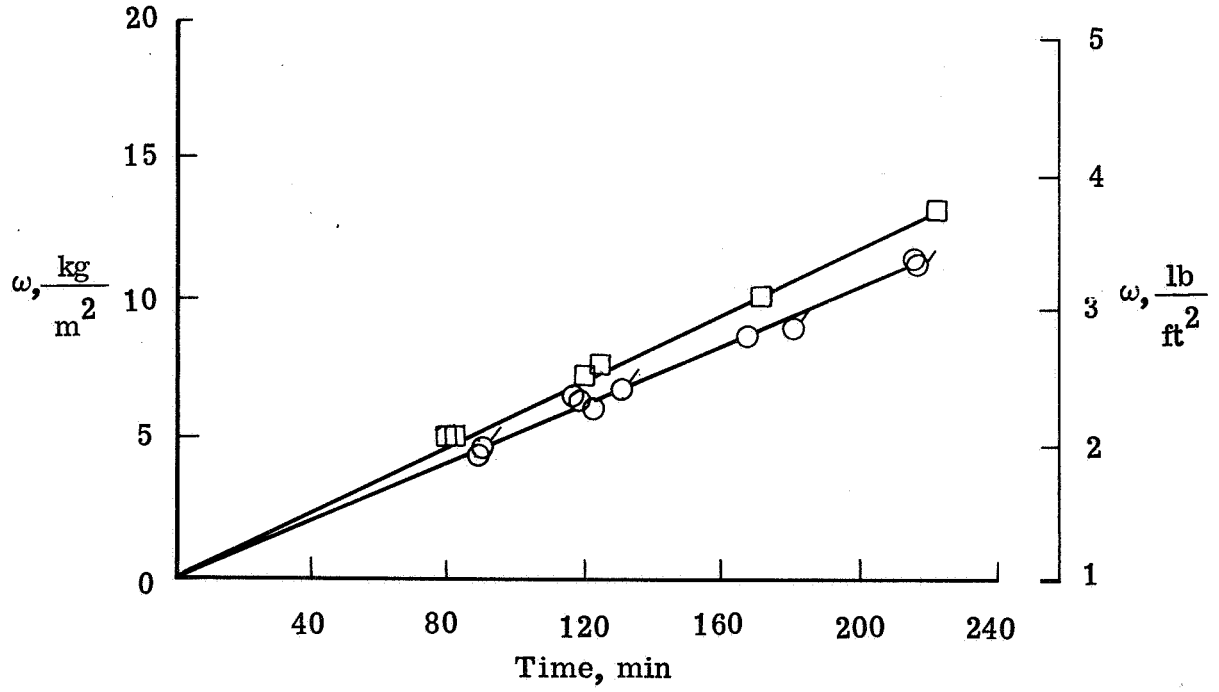

(b) Mass versus time.

Figure 10.- Effects of total pressure and cool-down rate on frost deposition for a 20-percent CO_2 mixture. L = 3.89 cm (1.53 in.); ρ_i = 20.8 kg/m^3 (1.3 lb/ft^3).

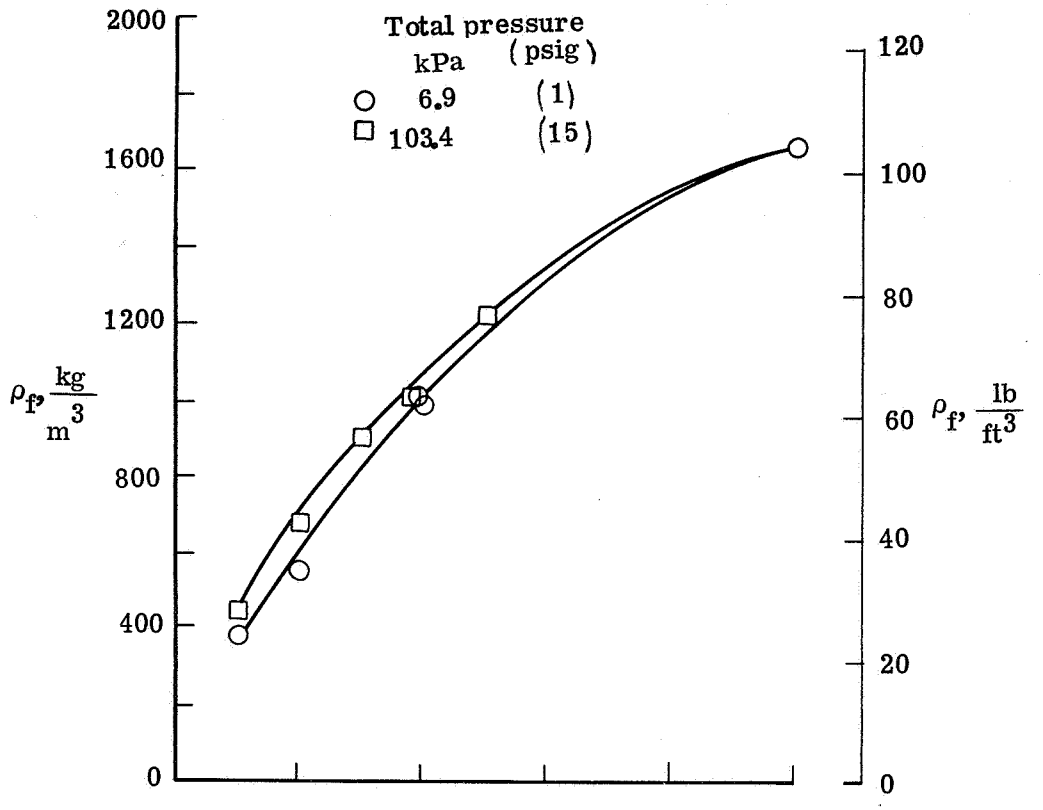

(a) Density versus percent CO_2.

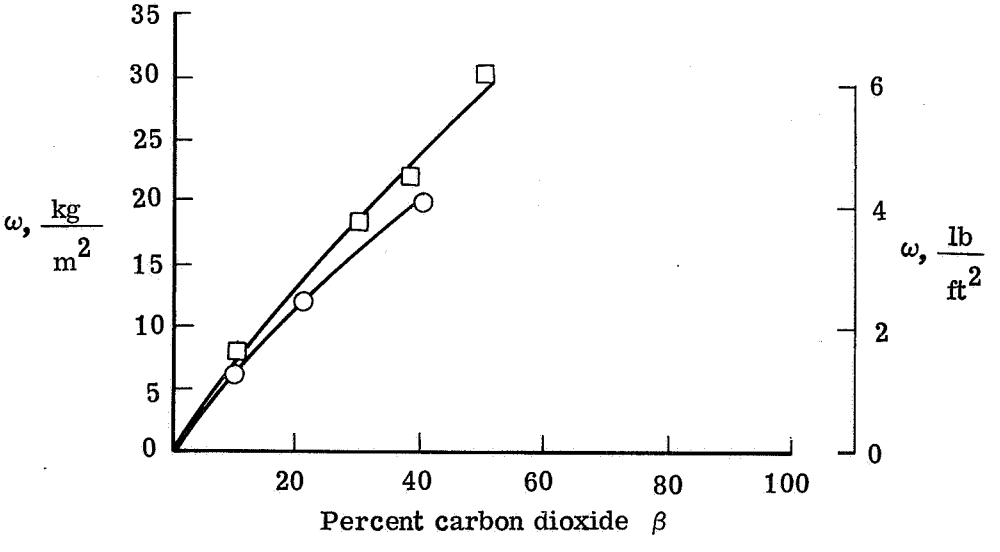

(b) Mass versus percent CO_2.

Figure 11.- Effect of total pressure on frost deposition for a frost-deposition time of 200 minutes. L = 3.89 cm (1.53 in.); ρ_i = 20.8 kg/m^3 (1.3 lb/ft^3).

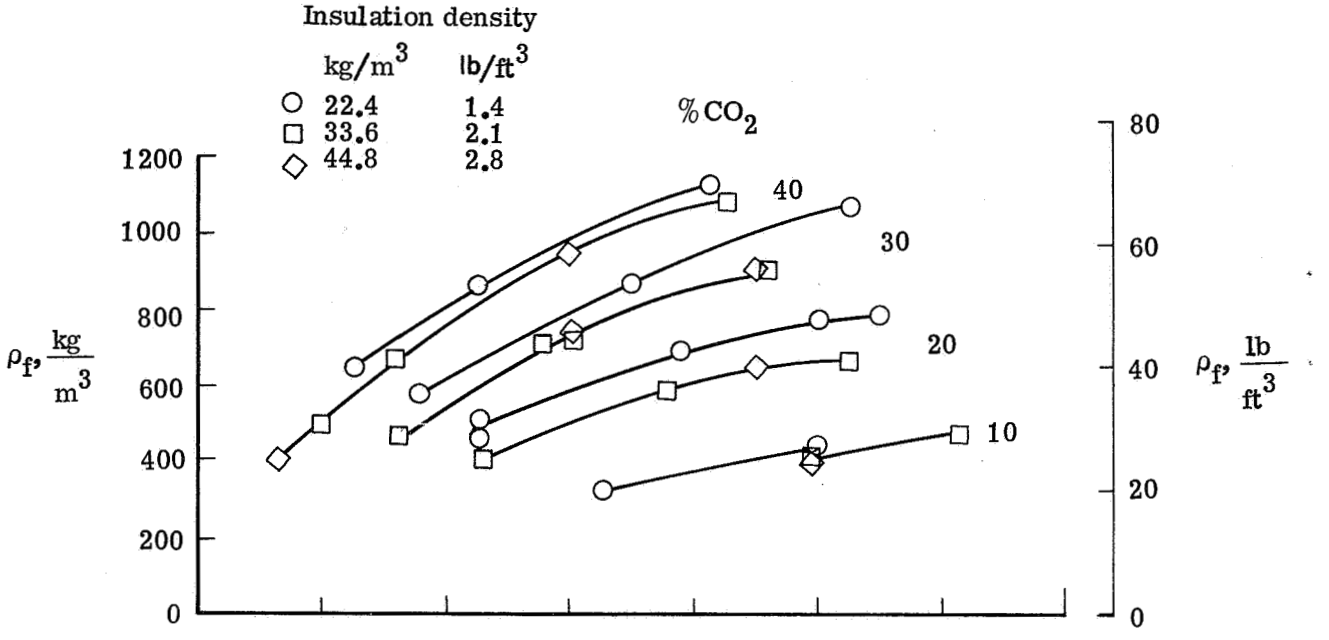

(a) Density versus time.

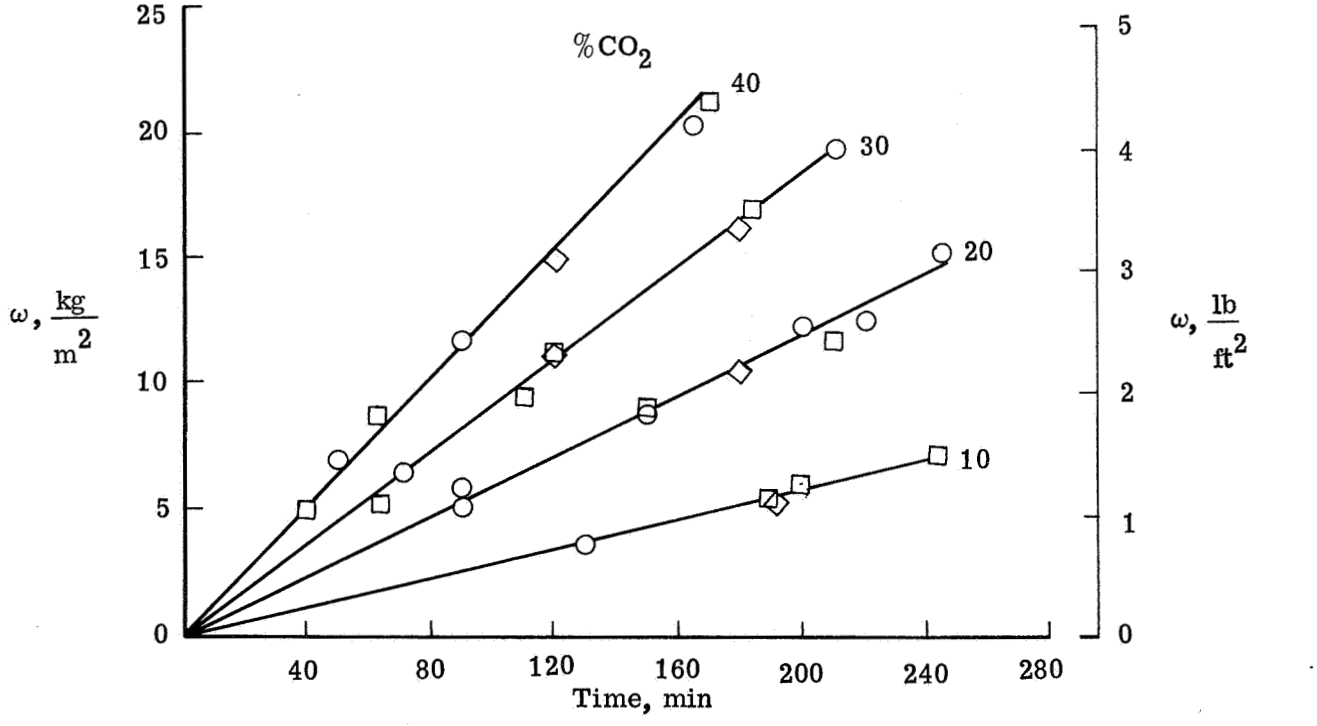

(b) Mass versus time.

Figure 12.- Effects of insulation density on frost deposition. L = 2.67 cm (1.05 in.).

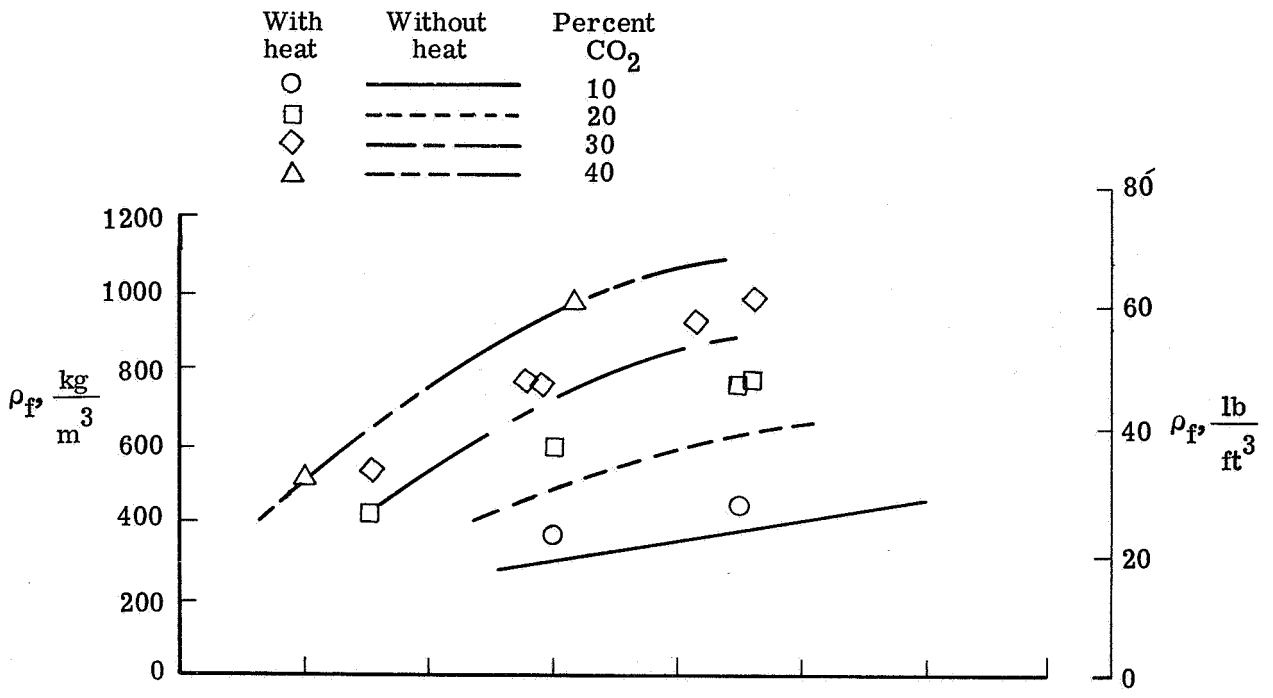

(a) Density versus time.

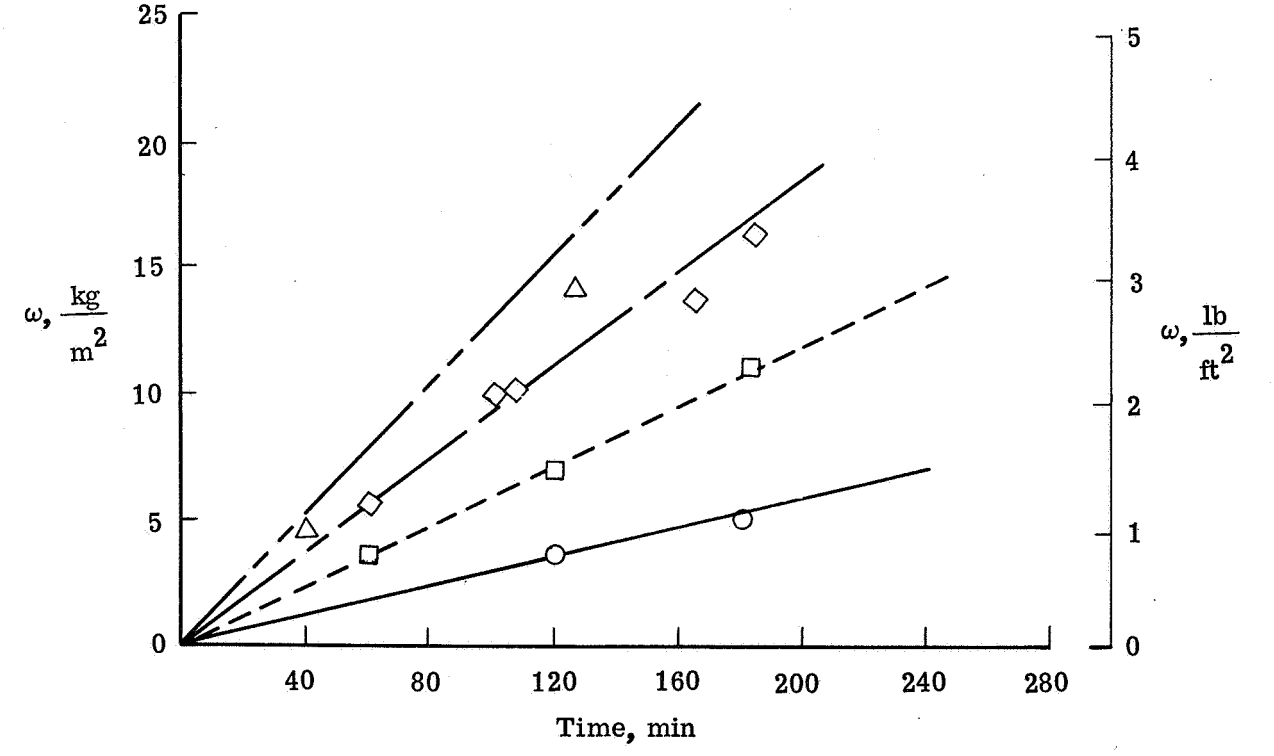

(b) Mass versus time.

Figure 13.- Effects of heating the outer tank on frost deposition. L = 2.67 cm (1.05 in.); ρ_i = 44.9 kg/m^3 (2.8 lb/ft^3).

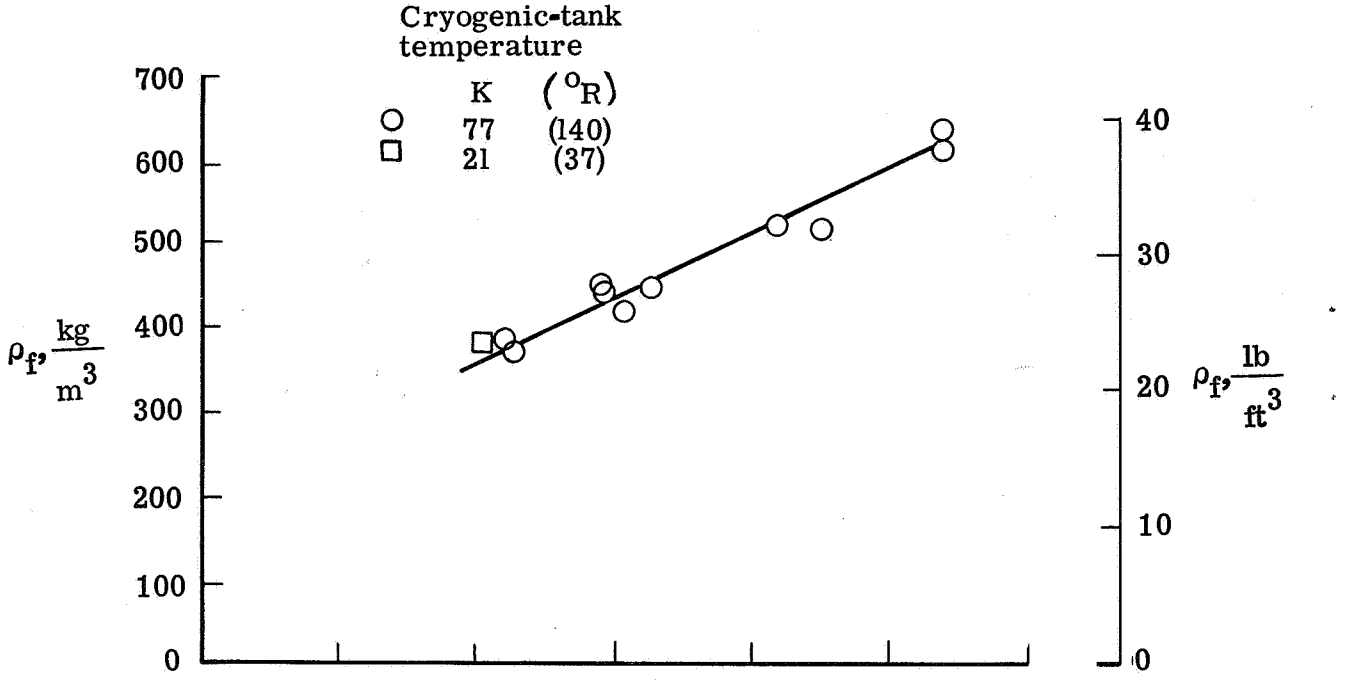

(a) Density versus time.

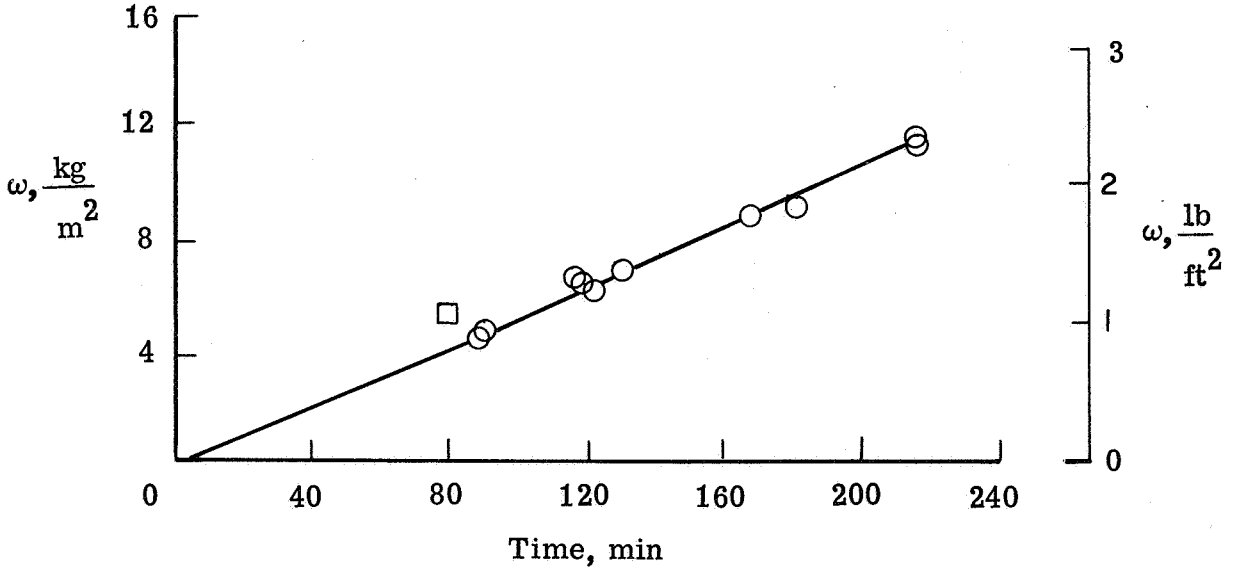

(b) Mass versus time.

Figure 14.- Effect of cryogenic-tank temperature on frost deposition for a 20-percent CO_2 mixture. L = 3.89 cm (1.53 in.); ρ_i = 20.8 kg/m³ (1.3 lb/ft³).

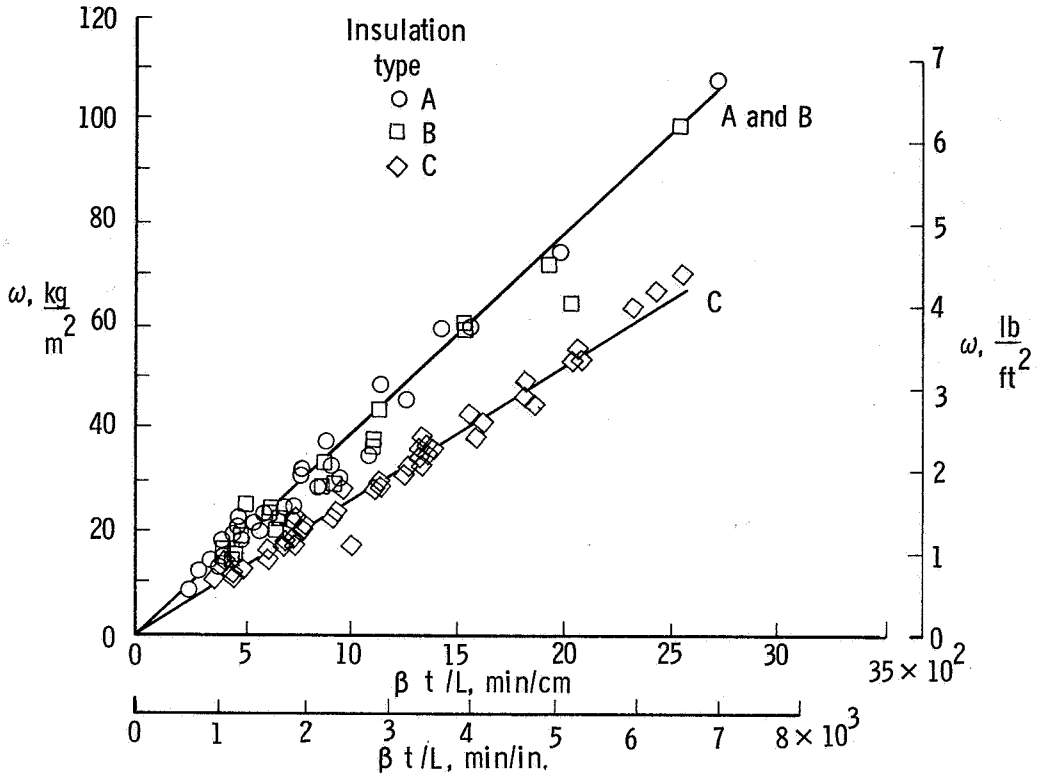

(a) Mass of frost deposited (ω) as a function of percent of CO_2 (β), time (t), and insulation thickness (L).

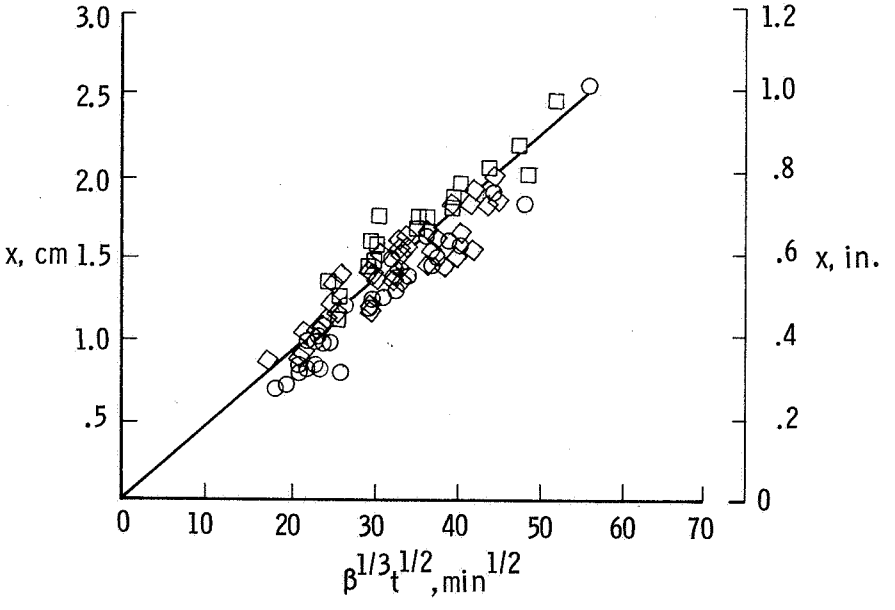

(b) Frost thickness (x) as a function of percent of CO_2 (β) and time (t).

Figure 15.- Correlation of data.

NASA-Langley, 1973 —— 33 L-8884